The FASEB Journal • Research Communication

Hematopoietic Akt2 deficiency attenuates the progression of atherosclerosis

Noemi Rotllan,*,†,‡ Aránzazu Chamorro-Jorganes,*,†,‡ Elisa Araldi,*,†,‡ Amarylis C. Wanschel,‡ Binod Aryal,*,†,‡ Juan F. Aranda,*,†,‡ Leigh Goedeke,*,†,‡ Alessandro G. Salerno,‡ Cristina M. Ramírez,*,†,‡ William C. Sessa,*,§ Yajaira Suárez,*,†,‡ and Carlos Fernández-Hernando*,†,‡,1

*Vascular Biology and Therapeutics Program, Yale University School of Medicine, New Haven, Connecticut, USA; †Integrative Cell Signaling and Neurobiology of Metabolism Program, Section of Comparative Medicine, Yale University School of Medicine, New Haven, Connecticut, USA; ‡Departments of Medicine, Leon H. Charney Division of Cardiology, and Cell Biology, New York University School of Medicine, New York, New York, USA; and §Department of Pharmacology, Yale University School of Medicine, New Haven, Connecticut, USA

ABSTRACT **Atherosclerosis is the major cause of death and disability in diabetic and obese subjects with insulin resistance. Akt2, a phosphoinositide-dependent serine-threonine protein kinase, is highly express in insulin-responsive tissues; however, its role during the progression of atherosclerosis remains unknown. Thus, we aimed to investigate the contribution of Akt2 during the progression of atherosclerosis. We found that germ-line *Akt2*-deficient mice develop similar atherosclerotic plaques as wild-type mice despite higher plasma lipids and glucose levels. It is noteworthy that transplantation of bone marrow cells isolated from $Akt2^{-/-}$ mice to $Ldlr^{-/-}$ mice results in marked reduction of the progression of atherosclerosis compared with $Ldlr^{-/-}$ mice transplanted with wild-type bone marrow cells. *In vitro* studies indicate that Akt2 is required for macrophage migration in response to proatherogenic cytokines (monocyte chemotactic protein-1 and macrophage colony-stimulating factor). Moreover, $Akt2^{-/-}$ macrophages accumulate less cholesterol and have an alternative activated or M2-type phenotype when stimulated with proinflammatory cytokines. Together, these results provide evidence that macrophage Akt2 regulates migration, the inflammatory response and cholesterol metabolism and suggest that targeting Akt2 in macrophages might be beneficial for treating atherosclerosis.—Rotllan, N., Chamorro-Jorganes, A., Araldi, E., Wanschel, A. C., Aryal, B., Aranda, J. F., Goedeke, L., Salerno, A. G., Ramírez, C. M., Sessa, W. C., Suárez, Y., Fernández-Hernando, C. Hematopoietic Akt2 deficiency attenuates the progression of atherosclerosis. *FASEB J.* 29, 597–610 (2015). www.fasebj.org**

Key Words: insulin resistance

ATHEROTHROMBOTIC VASCULAR DISEASE is the major cause of death and disability in diabetic and obese subjects with insulin resistance (1, 2). The risk of cardiovascular disease is increased in individuals with metabolic syndrome (MetS), which is characterized by insulin resistance without overt hyperglycemia (1, 2). Moreover, rapid weight gain during childhood leads to hyperinsulinemia and increased coronary artery disease risk in adult life. Part of the association between insulin resistance and cardiovascular disease is related to associated risk factors, including dyslipidemia (increased very LDL and reduced HDL) and hypertension (3). However, insulin resistance may have a proatherogenic effect at the level of inflammatory cells and in the arterial wall (4–8). Indeed, several studies have shown that insulin receptor-deficient macrophages promote a series of cellular events critical for advanced plaque progression. Moreover, mice lacking endothelial insulin signaling have a reduced endothelial-dependent vasodilatation and increased endothelial cell VCAM-1 expression, leading to a significant increase in atherosclerosis (7). These observations suggest that both hepatic and vessel wall insulin resistance promote atherosclerosis progression in mice.

The phosphoinositide-dependent serine-threonine protein kinase Akt [also known as protein kinase B (PKB)], has been proposed to be an intermediate in the signaling pathway by which insulin regulates muscle and fat glucose uptake, as well as hepatic gluconeogenesis (9, 10). In rodents and humans, there are 3 Akt isoforms (Akt1, Akt2, and Akt3), each encoded by a separate gene. Despite their similarity, gene knockout studies have shown that the 3 Akt isoforms have some nonredundant

Abbreviations: ABCA1, adenosine triphosphate-binding cassette transporter A1; ABCG1, adenosine triphosphate-binding cassette transporter G1; Ac-LDL, acetylated LDL; AKT/PKB, protein kinase B; ApoA1, apolipoprotein A1; ARG1, arginase 1; BMDM, bone marrow-derived monocytes; BMT, bone marrow transplantation; COX2, cyclooxygenase 2; DiI-Ox-LDL, DiI oxidized LDL; FoxO, Forkhead box O; GSK3, glycogen synthase kinase 3; HC, high cholesterol diet; LDLr, LDL receptor; MCP-1, monocyte chemotactic protein-1; M-CSF, macrophage colony-stimulating factor; MetS, metabolic syndrome; PAK1, p21-activated kinase 1; T2DM, type 2 diabetes mellitus; TG, triglyceride; WT, wild type

[1] Correspondence: Yale University School of Medicine, Amistad Research Building, Room 337C, 10 Amistad Street, New Haven, CT 06510. E-mail: carlos.fernandez@yale.edu

doi: 10.1096/fj.14-262097

This article includes supplemental data. Please visit *http://www.fasebj.org* to obtain this information.

functions (11–13). In the cardiovascular system, Akt1 plays an important role in the regulation of cardiac hypertrophy, angiogenesis, and apoptosis (4, 14–16). Most importantly, absence of Akt1 leads to severe atherosclerosis and occlusive coronary arterial disease (4, 5). The increased atherosclerosis observed in mice lacking Akt1 was associated with a significant reduction in NO and endothelial cell viability in athero-prone areas (4, 5). Moreover, a recent study has also shown that genetic deletion of the 3 genes encoding isoforms of the Forkhead box O (FoxO) transcription factors prevents atherosclerosis (8). FoxOs are phosphorylated and inactivated by Akt, suggesting that the enhanced atherosclerosis observed in the Akt1-null mice could be mediated by decreased eNOS activity and increased FoxO transcriptional activation (8). Paradoxically, the loss of the 3 FoxO isoforms in endothelial cells results in a significant down-regulation of Akt expression by an unknown mechanism. However, FoxO-deficient mice have a significant increase in NOS3 expression and enhanced eNOS-dependent arterial relaxation.

Although Akt1 regulates multiple functions in the cardiovascular system, Akt2 appears to be enriched in insulin-responsive tissues and has been specifically implicated in the metabolic actions of this hormone (11). In addition to regulating hepatic insulin signaling, it has also been reported that mice lacking *Akt2* have an impaired response to insulin in the vessel wall. This observation suggests that Akt2 activity might be important in controlling vascular function during insulin-resistant states observed in subjects with type 2 diabetes mellitus (T2DM) and MetS. Indeed, Akt2 mRNA levels inversely correlate with plasma insulin levels in circulating leukocytes isolated from insulin-resistant MetS patients (17). In addition to the regulation of insulin signaling, Akt2 also controls the macrophage inflammatory response. As such, genetic ablation of *Akt2* results in alternative activated M2 macrophages (18, 19), and *Akt2*-deficient mice are more resistant to LPS-induced endotoxin shock and to dextran sulfate sodium-induced colitis compared with wild-type (WT) mice. Taken together, these studies suggest that Akt2 might be a critical regulator during the progression of atherosclerosis by regulating insulin signaling in the liver and vessel wall and by controlling macrophage activation.

To assess the integrative role of Akt2 in atherogenesis *in vivo*, we generated mice lacking *Akt2* in the atheroprone $Ldlr^{-/-}$ mouse model. Surprisingly, we found that $Ldlr^{-/-}Akt2^{-/-}$ mice develop similar atherosclerotic plaques as $Ldlr^{-/-}$ mice despite having higher plasma lipids and glucose levels. It is noteworthy that transplantation of bone marrow cells isolated from $Akt2^{-/-}$ mice to $Ldlr^{-/-}$ mice results in marked reduction of the progression of atherosclerosis compared with $Ldlr^{-/-}$ mice transplanted with WT bone marrow cells. Mechanistically, we demonstrated that the absence of Akt2 in macrophages reduced foam cell formation, inflammatory activation, and migration. Thus, our study shows that the expression of Akt2 in macrophages plays a proatherogenic role by increasing lipid accumulation and enhancing monocyte/macrophage migration. These results also suggest that, although systemic inhibition of Akt2 could be deleterious for preventing atherosclerosis, specific Akt2 targeting in macrophages might be beneficial for treating atherosclerotic vascular disease.

MATERIALS AND METHODS

Animals

Male C57BL/6 (WT), $Ldlr^{-/-}Akt2^{-/-}$, and $Akt2^{-/-}$ mice were purchased from The Jackson Laboratory (Bar Harbor, ME, USA) and kept under constant temperature and humidity in a 12 h controlled dark/light cycle. Accelerated atherosclerosis was induced by feeding mice for 12 wk with a high cholesterol diet (HC) containing 1.25% cholesterol (D12108; Research Diets, Incorporated, New Brunswick, NJ, USA). All of the experiments were approved by the Institutional Animal Care Use Committee of New York University Medical Center and Yale University School of Medicine.

Lipids, lipoprotein profile, and glucose measurements

Mice were fasted for 12–14 h before blood samples were collected by retro-orbital venous plexus puncture. Then, plasma was separated by centrifugation and stored at −80°C. Total plasma cholesterol and triglycerides were enzymatically measured (Wako Pure ChemicalsTokyo, Japan) according to the manufacturer's instructions. The lipid distributions in plasma lipoprotein fractions were assessed by fast-performed liquid chromatography gel filtration with 2 Superose 6 HR 10/30 columns (Pharmacia Biotech, Uppsala, Sweden). Blood glucose was measured with a blood glucose meter (OneTouch Ultra; LifeScan, Incorporated, Milpitas, CA, USA) according to the manufacturer's instructions.

Histology, immunohistochemistry, and morphometric analyses

Mouse hearts were perfused with 10 ml PBS and were put in 10 ml 4% paraformaldehyde overnight. After incubation in paraformaldehyde, hearts were washed with PBS and left with PBS for 1 h. Next, hearts were put in 30% sucrose until the next day. Finally, hearts were embedded in OCT and frozen. Serial sections were cut at 8 μm thickness using a cryostat. Every third slide from the serial sections was stained with hematoxylin and eosin, and each consecutive slide was stained with Oil Red O for quantification of the lesion area. Aortic lesion size of each animal was obtained by averaging the lesion areas in 4 sections from the same mouse. Collagen content was assessed by Masson's trichrome of consecutive slides from serial sections. The fibrous cap and necrotic core area were measured as a percentage of the total plaque area from the 3 sections from the same mouse. CD68 staining was used as a macrophage marker using consecutive slides from serial sections. Apoptotic cells in lesions were detected by TUNEL after proteinase K treatment, using the In Situ Cell Death Detection kit, TMR red (Roche, Basel, Switzerland) according to the manufacturer's instructions. Nuclei were counterstained with DAPI for 10 min. The data are expressed as the number of TUNEL-positive cells per millimeter squared cellular lesion area. Proliferation cells in each lesion were detected by Ki67 staining (1:100; Abcam, Cambridge, MA, USA). Percentage of proliferating cells were calculated as the number of positive Ki67-labeled nuclei divided by the number of DAPI-stained nuclei. NIH ImageJ software (National Institutes of Health, Bethesda, MD, USA) was used for all the quantifications.

Bone marrow transplantation

Eight-week-old male *Ldlr*$^{-/-}$ mice were lethally irradiated with 1000 rads (10 Gy) using a cesium source 4 h before transplantation. Bone marrow was collected from femurs of donor WT or *Akt2*$^{-/-}$ mice. Each recipient mouse was injected with 2×10^6 bone marrow cells through retro-orbital injection. Four weeks after bone marrow transplantation (BMT), peripheral blood was collected by retro-orbital venous plexus puncture for PCR analysis of bone marrow reconstitution. For the atherosclerosis study, mice were fed with an HC diet for 12 wk beginning 4 wk after BMT and, on the basis of PCR genotyping, were fully chimeric.

Cell culture

Peritoneal macrophages from adult male WT or *AKT2*$^{-/-}$ mice were harvested by peritoneal lavage 4 d after intraperitoneal injection of thioglycollate (3% w/v). Cells were plated in RPMI 1640 medium supplemented with 10% fetal bovine serum, 100 U/ml penicillin, and 100 U/ml streptomycin. After 4 h, nonadherent cells were washed out, and macrophages were incubated in fresh medium containing DMEM, 10% fetal bovine serum, and 20% L-cell–conditioned medium for 24 h, and cells were maintained in culture as an adherent monolayer. Peritoneal macrophages were used for different experiments. Bone marrow-derived macrophages (BMDMs) from adult male WT or *AKT2*$^{-/-}$ mice were harvested and cultured in Iscove's Modified Dulbecco's medium (IMDM) supplemented with 20% L-cell–conditioned medium. After 7 d in culture, contaminating nonadherent cells were eliminated, and adherent cells were harvested for the assays.

Cholesterol efflux assays

Peritoneal macrophages from WT and *Akt2*$^{-/-}$ mice were seeded at a density of 1×10^6 cells per well 1 d prior to loading with 0.5 μCi/ml [^{3}H]cholesterol for 24 h with or without T0901317 (3 μmol/L) for 12 h.Cells then were washed twice with PBS and incubated in RPMI 1640 medium supplemented with 2 mg/ml fatty-acid free bovine serum albumin in the presence acetyl-coenzyme A acetyltransferase (ACAT) inhibitor (2 μmol/L; Novartis Corporation, New York, NY, USA) for 4 h prior to the addition of 50 μg/ml human ApoA1 in FAFA media. Supernatants were collected after 6 h and expressed as a percentage of [^{3}H] cholesterol in the media per total cell [^{3}H]cholesterol content (total effluxed [^{3}H]cholesterol + cell-associated [^{3}H]cholesterol). In some experiments, we silenced adenosine triphosphate-binding cassette transporter A1 (ABCA1) and adenosine triphosphate-binding cassette transporter G1 (ABCG1) expression by transfecting specific siRNA (Smart pool; GE Healthcare Dharmacon, Lafayette, CO, USA) using RNAimax (Invitrogen, Carlsbad, CA, USA) and following standard protocols.

Cell migration assays

Cell migration assays were performed with a modified Boyden chamber using Costar Transwell inserts (Corning, New York, NY, USA). The inserts from Costar Transwell were coated with 0.1% gelatin/PBS. BMDMs were serum-starved for 4 h. Solutions of monocyte chemotactic protein-1 (MCP-1; 100 ng/ml), macrophage colony-stimulating factor (M-CSF; 100 ng/ml), or 10% fetal bovine serum were prepared in RPMI 1640 medium and added to the bottom chambers. BMDMs (7×10^4) were added to the upper chambers. After 16 h of incubation at 37°C, cells on both sides of the membrane were fixed and stained with the Diff-Quik staining kit (Baxter Healthcare, Deerfield, IL, USA). Cells on the upper side of the membrane were removed with a cotton swab. The average number of cells per field on the lower side of the membrane from 4 high-power (×400) fields was counted.

Cellular cholesterol measurement and foam cell formation analysis

Peritoneal macrophages from WT and *Akt2*$^{-/-}$ mice were plated on 12-well plates and incubated with or without acetylated LDL (Ac-LDL; 120 μg/ml). After 24 h, intracellular cholesterol content was measured using the Amplex Red Cholesterol Assay Kit (Molecular Probes; Invitrogen), according to the manufacturer's instructions. For the foam cell formation assay, mouse peritoneal macrophages were grown on coverslips and treated with or without Ac-LDL (120 μg/ml) for 24 h.Cells were fixed with 4% paraformaldehyde for 20 min. After washing 3 times with PBS, cells were blocked for 30 min (PBS + bovine serum albumin 1%) and stained with Bodipy 493/503 for 30 min at room temperature. Next, cells were washed twice with 1× PBS and stained the nuclei with DAPI for 10 min to visualize the nuclei. Finally, cells were mounted on glass slides with Prolong-Gold (Life Technologies, Grand Island, NY, USA). All images were analyzed using confocal microscopy (Leica SP5 II; Leica Microsystems, Buffalo Grove, IL, USA) equipped with a 63× Plan Apo Lenses. All gains for the acquisition of comparable images were maintained constant. Analysis of different images was performed using ImageJ and Adobe Photoshop CS5.

Blood leukocyte analysis

Blood was collected by retro-orbital puncture in heparinized microhematocrit capillary tubes. Erythrocytes were lysed with ACK lysis buffer (155 mM ammonium chloride, 10 mM potassium bicarbonate, and 0.01 mM EDTA, pH 7.4). White blood cells were resuspended in 3% fetal bovine serum in PBS, blocked with 2 μg/ml FcgRII/III, and then stained with a cocktail of antibodies. Monocytes were identified as CD115^{hi} and subsets as Ly6-C^{hi} and Ly6-C^{lo}; neutrophils were identified as CD115^{lo}Ly6-C^{hi}Ly6-G^{hi}. The following antibodies were used (all from BioLegend, San Diego, CA, USA): FITC-Ly6-C (AL-21), PE-CD115 (AFS98), and APC-Ly6-G (1A8). CCR2 expression was assessed using a CCR2-conjugated antibody (475301; R&D Systems, Minneapolis, MN, USA).

Hematopoietic stem cell analysis

Bone marrow was harvested from femurs and tibias. Cells were blocked with 2 μg/ml Alexa Fluor-700–conjugated FcgRII/III and stained for lineage markers [B220 (RA3-6B2), CD11b (M1/70), Gr-1 (RB6-8C5), TER-119, CD8a (53-6.7), CD4 (RM4-5), IL7Ra (A7R34), all APC-Cy7 conjugated], FITC-ckit (2B8), PE-Cy7-Sca1 (D7), and APC-CD34 (RAM34). Common myeloid progenitor cells were identified as Lin$^-$/ckit$^+$ Sca1$^-$/CD34^{int}, FcgRII/III^{int}, whereas granulocyte-macrophage progenitor cells were identified as Lin$^-$/ckit$^+$ Sca1$^-$/CD34^{int}, FcgRII/III^{hi}. All antibodies were from BioLegend. Flow cytometry was performed using a BD LSRII. All flow cytometry data were analyzed using Tree Star software (FlowJo, Ashland, OR, USA).

DiI-Ox-LDL uptake and binding assays

DiI-Ox-LDL lipoproteins were oxidized and labeled with the fluorescent probe DiI. For the uptake assays, mouse peritoneal macrophages were washed once in 1× PBS and incubated in

fresh media containing DiI-Ox-LDL (30 μg/ml cholesterol) for 2 h at 37°C. For the binding assays, cells were incubated for 15 min at 4°C to stop membrane internalization.Cells then were treated or not with fresh media containing DiI-Ox-LDL (30 μg/ml cholesterol) for 1 h and 30 min at 4°C. At the end of the incubation period, cells were washed, and 1 ml RPMI 1640 medium, 10% fetal bovine serum was added for 15 min at 37°C to allow the internalization. Finally, in both assays, cells were washed and resuspended in 1 ml PBS and analyzed by flow cytometry (FACScalibur; Becton Dickinson, San Diego, CA, USA). The results are expressed in terms of specific median intensity of fluorescence after subtracting the autofluorescence of cells incubated in the absence of DiI-LDL.

M1 and M2 polarization assay

BMDMs from WT or *Akt2*$^{-/-}$ mice were stimulated for 8 h with IL-4 (15 ng/ml; R&D) or LPS (10 ng/ml; Sigma-Aldrich, St. Louis, MO, USA) and IFN-γ (20 ng/ml; R&D) to polarize macrophages to M2 or M1, respectively. At the end of the treatment, cells were extensively washed with 1× PBS, and RNA and protein were isolated.

BMDM immunofluorescent staining and confocal imaging

BMDMs from WT or *Akt2*$^{-/-}$ mice were seed onto glass coverslips in macrophage growth medium. Cells were serum-starved for 4 h and then stimulated with 50 ng/ml M-CSF (R&D Systems) for 15 min. BMDMs were fixed with 4% paraformaldehyde in PBS for 10 min at room temperature.Cells then were permeabilized with 0.2% Triton X-100 in PBS for 5 min and stained for Rac (BD Biosciences). Cells were then incubated with fluorescent-labeled secondary antibody (Alexa Fluor 594 anti-mouse; Invitrogen). F-actin was visualized with FITC-conjugated phalloidin (Invitrogen). Nuclei were counterstained with DAPI for 10 min. Finally, cells were mounted onto glass slides with Prolong-Gold (Life Technologies). Images of cells were acquired using a Leica TCS SP5 confocal microscope with a 63× Plan Apochromat objective. All images were taken using Sequential Scan application (Leica), so the overlap of emission spectra of the fluorochromes was reduced.

Akt substrate phosphorylation in BMDMs after M-CSF stimulation

BMDMs from WT or *Akt2*$^{-/-}$ mice were seeded onto 6-well plates. Cells were serum- and M-CSF-starved for 8 h and then stimulated with 50 ng/ml M-CSF (R&D Systems) at different time points. Cells were washed, and protein extraction was performed.

Rac activity assay

Pull-down of GTP-bound Rac was performed by incubating cell lysates with GST-fusion protein containing the p21-binding domain of p21-activated kinase 1 (PAK-1) bound to glutathione agarose for 1 h at 4°C. The amount of GTP-bound Rac was examined by immunoblotting using a Rac monoclonal antibody (EMD Millipore Corporation, Billerica, MA, USA).

Western blotting

Tissue or cells were lysed in ice-cold buffer containing 50 mM Tris-HCl, pH 7.5, 125 mM NaCl, 1% Nonidet P-40, 5.3 mM NaF, 1.5 mM NaP, 1 mM orthovanadate, and 1 mg/ml protease inhibitor cocktail (Roche) and 0.25 mg/ml Pefabloc, 4-(2-aminoethyl)-benzenesulfonyl fluoride hydrochloride (AEBSF) (Roche). Tissue or cell lysates were rotated at 4°C for 1 h before the insoluble material was removed by centrifugation at 12,000 × *g* for 10 min. After normalizing for equal protein concentration, cell lysates were resuspended in SDS sample buffer before separation by SDS-PAGE. Western blots were performed using the following antibodies: rabbit polyclonal antibodies against phospho-Akt (Ser473) (1:1000), Akt1 (1:1000), Akt2 (1:1000), Akt (1:1000), phospho-ERK (Thr202/Tyr204) (1:1000), phospho-PAK1 (Ser199/204)/PAK2 (Ser192/197) (1:1000), PAK (1:1000), phospho-GSK-3-β (Ser9) (1:1000), glycogen synthase kinase 3 (GSK-3)-β (1:1000), phospho-FoxO1 (Ser256) (1:1000), FoxO1 (1:1000), and NOS-2 (1:1000). Mouse monoclonal antibodies against ERK (1:1000) and phospho-Akt (Thr308) (1:1000) were obtained from Cell Signaling Technology (Danvers, MA, USA), and a mouse monoclonal antibody against ABCA1 (1:1000) and rabbit monoclonal antibody against CD36 (1:1000) were both from Abcam. Furthermore, a rabbit polyclonal antibody against ABCG1 (1:500) was from Novus (St. Charles, MO, USA), rabbit polyclonal antibodies against cyclooxygenase 2 (COX2; 1:1000) were from Cayman Chemicals (Ann Arbor, MI), a goat polyclonal antibody against SR-A (1:1000) was from Santa Cruz Biotechnology (Santa Cruz, CA, USA), and mouse monoclonal antibody against HSP-90 was from BD Biosciences. Secondary antibodies were fluorescence-labeled antibodies from LI-COR Biotechnology. Protein bands were visualized using the Odyssey Infrared Imaging System (LI-COR Biosciences, Lincoln, NE, USA). Densitometry analysis of the gels was carried out using NIH ImageJ software (http://rsbweb.nih.gov/ij/).

RNA isolation and quantitative real-time PCR

Total RNA from mouse aortas was isolated using the Bullet Blender Homogenizer (Next Advance, Averill Park, NY, USA) in TRIzol reagent (Invitrogen) according to the manufacturer's protocol. Total RNA from BMDMs was isolated using TRIzol reagent. One microgram of total RNA was reverse transcribed using the iScript RT Supermix (Bio-Rad, Hercules, CA), following the manufacturer's protocol. Quantitative real-time PCR was performed in triplicate using iQ SYBR green Supermix (Bio-Rad) on a Real-Time Detection System (Eppendorf). The mRNA level was normalized to GAPDH as a housekeeping gene. Quantitative real-time PCR was performed in triplicate using miScript SYBR Green (QIAGEN, Valencia, CA) on a Real-Time Detection System (Eppendorf, Hauppauge, NY, USA). The following mice primer sequences were used: CD68, 5′-CCAATTCAGGGTGGAAGAAA-3′ and 5′-CTCGGGCTCTGATGTAGGTC-3′; ESEL, 5′-AGCTACCCATGGAACACGAC-3′ and 5′-CGCAAGTTCTCCAGCTGTT-3′; GAPDH, 5′-AACTTTGGCATTGTGGAAGG-3′ and 5′-ACACATTGGGGGTAGGAACA-3′; ICAM, 5′-CTCGGAGACATTAGAGAACAATGC-3′ and 5′-GGGACCACGGAGCCAATT-3′; NOS2, 5′-CAGCTGGGCTGTACAAACCTT-3′ and 5′-CATTGGAAGTGAAGCGTTTCG-3′; IL-6, 5′-AGTTGCCTTCTTGGGACTGA-3′ and 5′-TCCACGATTTCCCAGAGAAC-3′; MAC-2 5′-AGGAGAGGGAATGATGTTGCC-3′ and 5′-GGTTTGCCACTCTCAAAGGG-3′; TNFα, 5′-CCCTCACACTCAGATCATCTTCT-3′and 5′-GCTACGACGTGGGCTACAG-3′; VCAM-1, 5′-GCGTTTAGTGGGCTGTCTATCTG-3′ and 5′-CTGAATACAAAACGATCGCTCAA-3′; MCP-1 (CCL2), 5′-TCTGGGCCTGCTGTTCAC-3′ and 5′-GTGAATGAGTAGCAGCAGGTGAGT-3′; CCL3, 5′-AGCTGTGGTATTCCTGACCA-3′ and 5′-GGCAGGAAATCTGAACGTGA-3′; and CCL5, 5′-AGAGGACTCTGAGACAGCAC-3′ and 5′-CCTTCGAGTGACAAACACGA-3′.

Statistical analysis

Data are presented as mean ± SEM (*n* is noted in the figure legends), and the statistical significance of the differences was

evaluated with the Student's *t* test. Significance was accepted at the level of $P < 0.05$. Data analysis was performed using GraphPad Prism 6.0a software (GraphPad Software Incorporated, San Diego, CA, USA).

RESULTS

Akt2 deficiency results in hyperglycemia and dyslipidemia

Dyslipidemia and hyperglycemia are important risk factors that predispose an individual to develop coronary artery disease (2, 20). Akt2 is the predominant isoform expressed in insulin target tissues including the liver, adipose tissue, and muscle and *Akt2*-null mice exhibit glucose intolerance and a mild diabetic phenotype (11). Therefore, we initially analyzed the impact of Akt2 deficiency on multiple metabolic parameters in the atheroprone $Ldlr^{-/-}$ mice. *Akt2* genetic deletion results in decreased body weight after feeding mice with an HC diet for 12 wk (Fig. 1*A*). It is noteworthy that circulating levels of glucose, triglycerides (TGs), and cholesterol were significantly higher in mice lacking Akt2 (Fig. 1*B–D*). Likewise, the cholesterol and TG distribution were increased in very LDL fractions isolated by fast protein liquid chromatography from $Akt2^{-/-}Ldlr^{-/-}$ compared with $Ldlr^{-/-}$ mice (Fig. 1*E–H*). These findings demonstrate that the absence of Akt2 results in hyperglycemia and dyslipidemia in $Ldlr^{-/-}$-deficient mice.

Germ-line Akt2 deletion does not influence the progression of atherosclerosis

To study the functional role of Akt2 during the progression of atherosclerosis, we fed double mutant $Akt2^{-/-}Ldlr^{-/-}$ and corresponding $Ldlr^{-/-}$ mice with an HC diet for 12 wk and assessed atheroma formation in the aortic root by immunohistochemistry. As shown in Fig. 2*A*, the absence of Akt2 does not alter the size of the atherosclerotic plaques in the aortic sinus. Moreover, the necrotic core, fibrous cap, and macrophage content in the atherosclerotic lesions were similar between both groups of mice (Fig. 2*B–D*). Collectively, these results demonstrate that global Akt2 deficiency does not influence atherogenesis. We next assessed whether absence of Akt2 reduces Akt activation in the arterial wall in $Ldlr^{-/-}$ mice fed an HC diet for 12 wk. The results showed that the total Akt expression and phosphorylation (Ser473) were significantly reduced in $Akt2^{-/-}Ldlr^{-/-}$ mice compared with $Ldlr^{-/-}$ mice (Fig. 2*E*, band densitometry analysis in the bottom panel). Accordingly, the phosphorylation of FoxO1, an Akt downstream target, was also significantly decreased in aorta lysates isolated from *Akt2*-deficient mice (Fig. 2*E*, quantified in the bottom panel). It is surprising that the activation of other Akt downstream targets, such as GSK-3 was not affected in mice lacking *Akt2* (Fig. 2*E*), suggesting different substrate specificity for the 3 Akt isoforms. In addition to Akt, ERK activation was also significantly inhibited in $Akt2^{-/-}Ldlr^{-/-}$ mice compared with $Ldlr^{-/-}$ mice (Fig. 2*E*, band densitometry analysis in the bottom panel).

$Akt2^{-/-}$ bone marrow recipients develop smaller and less inflammatory atherosclerotic plaques

The finding that *Akt2*-null mice develop similar lesions despite of having higher circulating glucose and lipid levels was unexpected. Because macrophages and other bone marrow-derived cells play a central role during the progression of atherosclerosis, we wondered whether Akt2 might be atheroprotective. Therefore, to assess the contribution of Akt2 in bone marrow-derived cells during atherogenesis, we performed BMT experiments. In contrast to the global deficient Akt2 mice, the $Akt2^{-/-}$ bone marrow recipient mice had similar body weight and plasma lipid levels as WT recipient mice (Fig. 3*A–E*). Of note, mice receiving Akt2-deficient bone marrow developed significantly smaller lesions than mice transplanted with WT bone marrow cells (Fig. 3*F*, upper panels). Importantly, macrophage accumulation in atherosclerotic plaques was markedly reduced in $Ldlr^{-/-}$ mice transplanted with $Akt2^{-/-}$-deficient bone marrow compared with WT recipient mice (Fig. 3*F*, lower panels).

To determine the mechanism by which absence of Akt2 results in a marked reduction of macrophage accumulation in the artery wall, we initially analyzed the cellular composition of peripheral blood and bone marrow in Akt2-deficient mice. Peripheral blood counts showed similar number of white cells between both groups of mice (Supplemental Fig. 1*A*). These findings were corroborated by flow cytometry analysis of peripheral blood that showed similar relative and absolute numbers of neutrophils and monocytes (Supplemental Fig. 1*B*). Moreover the numbers of $Ly6C^{hi}$ monocytes, a key population associated with the progression of atherosclerosis in mice, was similar in $Akt2^{-/-}$ and WT mice (Supplemental Fig. 1*B*, quantification right panel). As expected by the similar cellular blood composition observed in both group of mice, bone marrow analysis revealed that the abundance of hematopoietic stem and progenitor cells, common myeloid progenitor, and granulocyte-macrophage progenitor cells were similar in both groups of mice (Supplemental Fig. 1*C*, quantification in right panel). We next examined whether the reduction in macrophage accumulation observed in mice transplanted with $Akt2^{-/-}$ bone marrow cells was caused by an increase apoptosis or reduced proliferation. We found similar proliferation rates in both groups of mice (Supplemental Fig. 2*A*) but a significant increase in apoptosis in mice transplanted with Akt2-deficient bone marrow (Supplemental Fig. 2*B*).

We next determined the effect of Akt2 deficiency in bone marrow-derived cells on vascular inflammation by assessing the expression of inflammation markers from the aortas of $Ldlr^{-/-}$ mice transplanted with WT or $Akt2^{-/-}$-deficient bone marrow after 12 wk on an HC diet by quantitative RT-PCR. As seen in Fig. 3*G*, the expression of several adhesion molecules (SELE, VCAM-1, and IL-6) and chemokines that regulates monocyte/macrophage infiltration in the artery wall (CCL2, CCL3, and CCL5) were significantly reduced in $Ldlr^{-/-}$ mice transplanted with $Akt2^{-/-}$-deficient bone marrow. As expected by the marked reduction in

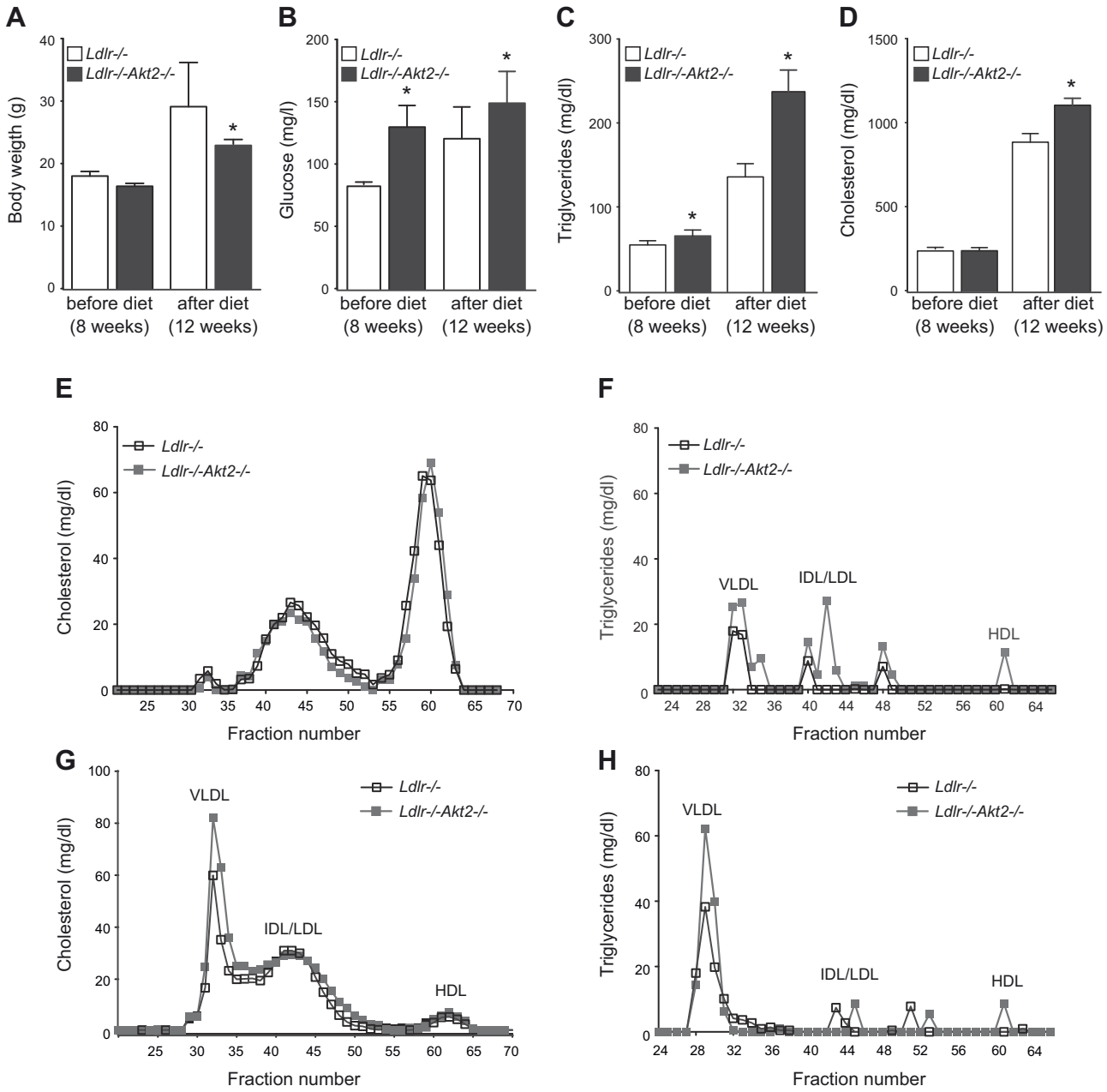

Figure 1. Dyslipidemia and hyperglycemia in male $Ldlr^{-/-}$ and $Ldlr^{-/-}Akt2^{-/-}$ mice after a high cholesterol diet. Body weight (*A*), glucose (*B*), TG (*C*), and cholesterol (*D*) levels from 8-wk-old male $Ldlr^{-/-}$ and $Akt2^{-/-}Ldlr^{-/-}$ mice before and after 12 wk on a high-cholesterol (HC) diet. All data represent the mean ± SEM ($Ldlr^{-/-}$, $n = 10$; $Akt2^{-/-}Ldlr^{-/-}$, $n = 14$). *$P < 0.05$ compared with $Ldlr^{-/-}$. Cholesterol (*E, G*) and TG lipoprotein (*F, H*) profiles from pooled plasma ($n = 4$) from male $Ldlr^{-/-}$ and $Akt2^{-/-}Ldlr^{-/-}$ mice before (*E, F*) and after (*G, H*) 12 wk on HC diet.

macrophage accumulation in atherosclerotic plaques from $Akt2^{-/-}$ BMT mice, CD-68 and MAC-2 expression was also significantly reduced (Fig. 3*G*). The decreased inflammation and macrophage accumulation was associated with a marked reduction in Akt phosphorylation at both sites Ser473 and Thr308 (but not Akt levels) (Fig. 3*H*). Moreover, FoxO1 and ERK phosphorylation was also reduced in $Ldlr^{-/-}$ mice transplanted with $Akt2^{-/-}$ bone marrow (Fig. 3*H*). Collectively, these results strongly suggest that absence of Akt2 in bone marrow-derived cells protects against the progression of atherosclerosis in mice.

Loss of Akt2 reduces macrophage foam cell formation

Accumulation of cholesterol in macrophages during early steps of the atherosclerotic plaque formation is a critical step during the development of this disease (20, 21). To investigate whether Akt2 regulates lipid accumulation in macrophages, we cultured mouse peritoneal macrophages in the presence of Ac-LDL for 24 h. Bodipy staining revealed a significant reduction of neutral lipid accumulation in macrophages lacking Akt2 compared with WT macrophages (Fig. 4*A*). Similar results were observed when we assessed the total cholesterol content

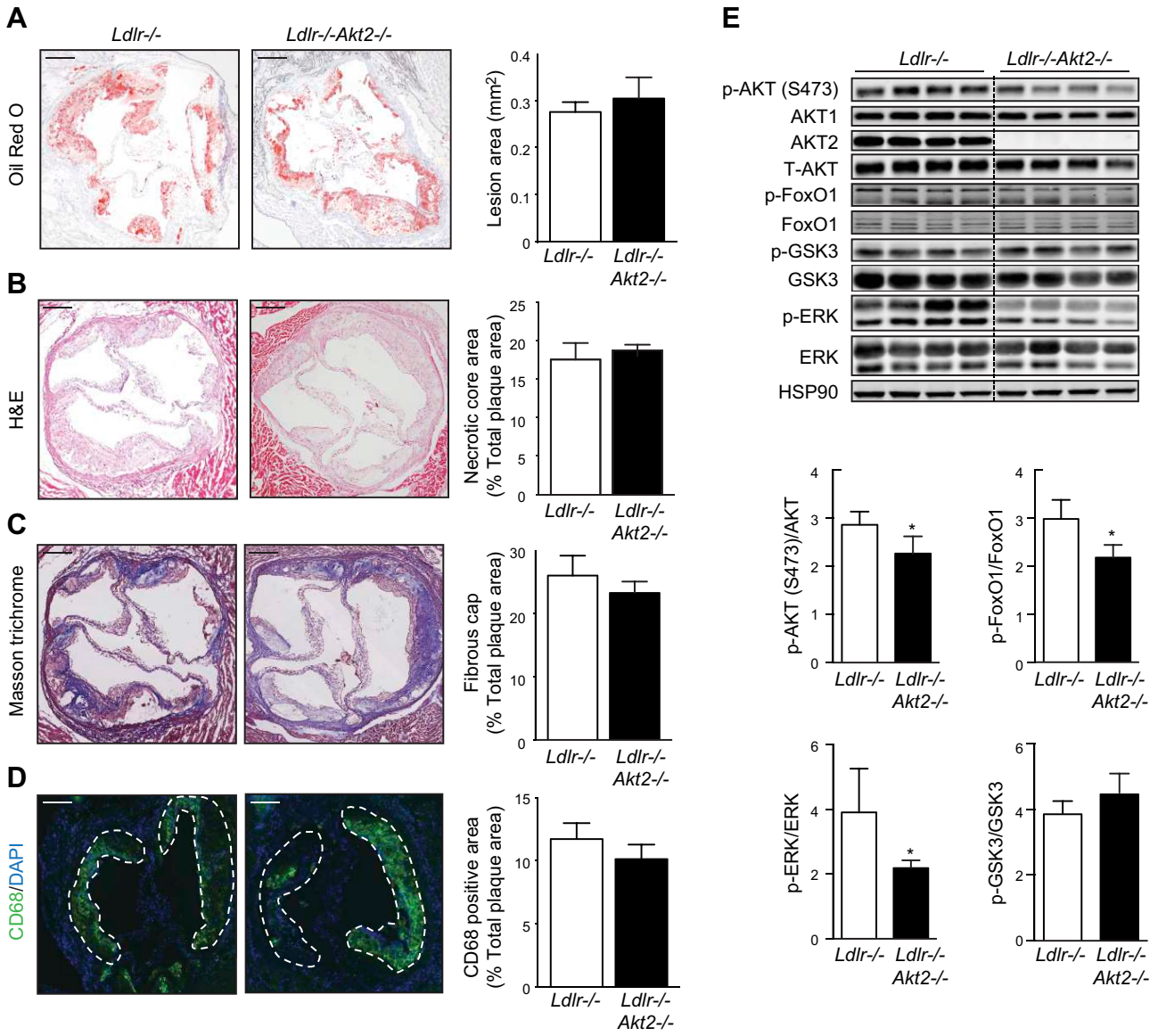

Figure 2. Global deficiency of AKT2 does not influence atherogenesis. Representative histologic analysis of cross-sections from the aortic sinus stained with Oil Red O (ORO) (*A*), hematoxylin and eosin (H&E) (*B*), Masson's trichrome (MT) (*C*), and CD68 and DAPI (*D*). Quantification of the lesion area, fibrous cap, necrotic core, and macrophage content is represented in the right panels. All data represent the mean ± SEM ($Ldlr^{-/-}$, $n = 10$; $Ldlr^{-/-}Akt2^{-/-}$, $n = 14$). Scale bar, 400 μm. (*E*) Representative Western blot analysis of AKT isoforms and downstream AKT targets from aortic lysates of male $Ldlr^{-/-}$ and $Akt2^{-/-}Ldlr^{-/-}$ mice. HSP90 was used as a loading control. Band densitometry is shown in the bottom panels. $^*P < 0.05$ compared with $Ldlr^{-/-}$.

in cells (Fig. 4*B*). We next investigated whether the reduced lipid accumulation observed in the absence of Akt2 was due to a reduced uptake of modified lipoproteins or increased cellular cholesterol efflux. Flow cytometry analysis revealed no differences in the binding and uptake of lipoproteins between both groups of mice (Fig. 4*C*, *D*). However, cellular cholesterol efflux to ApoA1 and fetal bovine serum was slightly increased in Akt2-deficient macrophages (Fig. 4*E*, *F*). To assess whether the different cholesterol efflux capacity observed in Akt2-deficient macrophages was associated with the decrease foam cell formation, we silenced the ABC transporters (ABCA1 and ABCG1) that mediate cholesterol efflux in macrophages and analyzed lipid accumulation after cholesterol loading with Ac-LDL. The results show that silencing ABCA1 expression results in similar cholesterol accumulation in WT and $Akt2^{-/-}$ macrophages, suggesting that ABCA1-dependent efflux activity mediates the decrease in lipid accumulation observed in Akt2-deficient macrophages (Supplemental Fig. 3). We further analyzed the expression of the scavenger receptors that regulate the uptake of modified lipoproteins (CD36 and SRA) and transporters that control the cellular cholesterol efflux (ABCA1 and ABCG1). As expected by similar lipoprotein uptake, CD36 and SRA expression was comparable between both groups of macrophages (Fig. 4*G*, band densitometry analysis in the right panel). ABCA1 expression was also similar in WT and Akt2 macrophages, but ABCG1 appeared to be slightly up-regulated in Akt2-deficient macrophages.

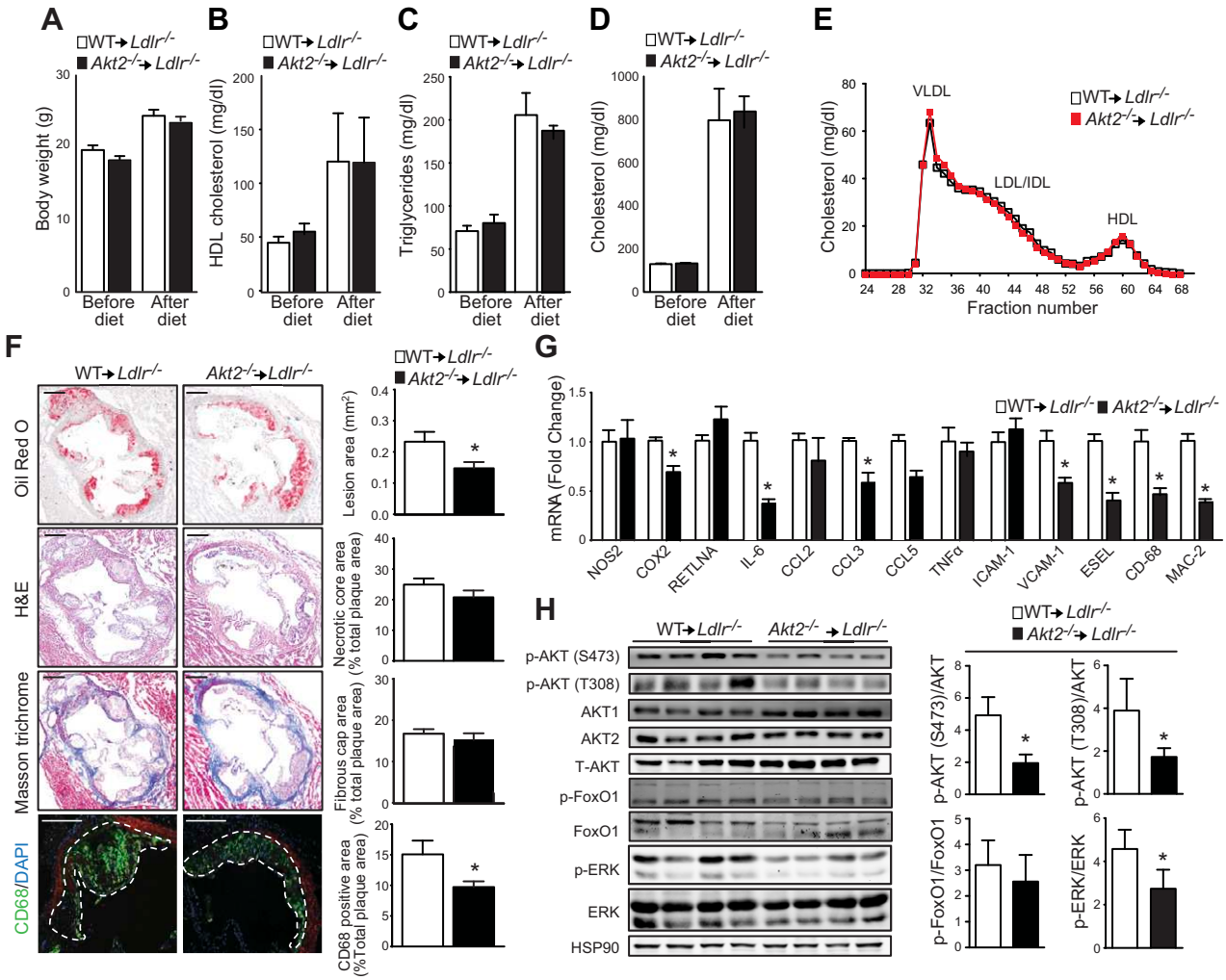

Figure 3. $Akt2^{-/-}$ bone marrow recipients develop smaller and less inflammatory atherosclerotic plaques. Body weight (*A*), HDL cholesterol (*B*), TG (*C*), and cholesterol (*D*) levels from $Ldlr^{-/-}$ chimeras with WT *or* $Akt2^{-/-}$ bone marrow before and after 12 wk on an HC diet. All data represent the mean ± SEM (WT, $n = 8$; $Akt2^{-/-}$, $n = 8$). (*E*) Cholesterol lipoprotein profile from pooled plasma ($n = 4$) from $Ldlr^{-/-}$ chimeras with WT *or* $Akt2^{-/-}$ bone marrow after 12 wk on an HC diet. (*F*) Representative histologic analysis of cross sections from the aortic sinus from $Ldlr^{-/-}$ chimeras with WT *or* $Akt2^{-/-}$ bone marrow after 12 wk on an HC diet with Oil Red O (ORO), hematoxylin and eosin (H&E), Masson trichrome, and CD68/α-SMC actin/DAPI. Quantification of the lesion area, fibrous cap, necrotic core, and macrophage content are represented in the right panels. Scale bar, 400 μm. (*G*) Aorta expression profile of atherosclerotic-related genes assessed by real-time quantitative PCR. Four independent quantitative PCR reactions were carried out for each condition. The fold change for each gene of WT mice compared with $Akt2^{-/-}$ mice. The data represent the mean ± SEM. (*H*) Representative Western blot analysis of downstream targets of Akt from aortic lysates of male $Ldlr^{-/-}$ chimeras with *WT or* $Akt2^{-/-}$ bone marrow after 12 wk on an HC diet. HSP90 was used as a loading control. Band densitometry is shown in the right panels. $^*P < 0.05$ compared with WT.

Altogether, these results demonstrate that the absence of Akt2 reduces lipid accumulation in macrophages.

Akt2 deficiency results in alternative activated or M2 macrophages

Activated macrophages are described as classically activated (M1 type) or alternatively activated (M2 type), depending on their response to proinflammatory stimuli and the expression of genetic markers such as NOS2, IL-12, COX2, ARG1, RETLNA, MRC1, and YM-1 (22, 23). Both macrophage subsets are present in atherosclerotic plaques, and it is thought that M1 macrophages promote plaque inflammation, whereas M2 macrophages resolve plaque inflammation (24). To determine whether Akt2 deficiency influences macrophage polarization, we incubated mouse BMDMs in the presence of LPS and IFN-γ (to stimulate the M1 phenotype) or IL-4 (to stimulate the M2 phenotype). The results showed that $Akt2^{-/-}$ macrophages treated with LPS/IFN expressed lower mRNA and protein levels of COX2 compared with WT macrophages (Fig. 5*A, B*). NOS2 protein expression was also markedly reduced (Fig. 5*B*). Interestingly, the absence of Akt2 significantly increased the expression of M2 markers, including ARG1, RETLNA, and YM-1 (Fig. 5*C*). Similar results were observed in BMDMs previously loaded with cholesterol (Supplemental Fig. 4*A, B*). Altogether, these results suggest that Akt2 deficiency results in M2 polarization of macrophages.

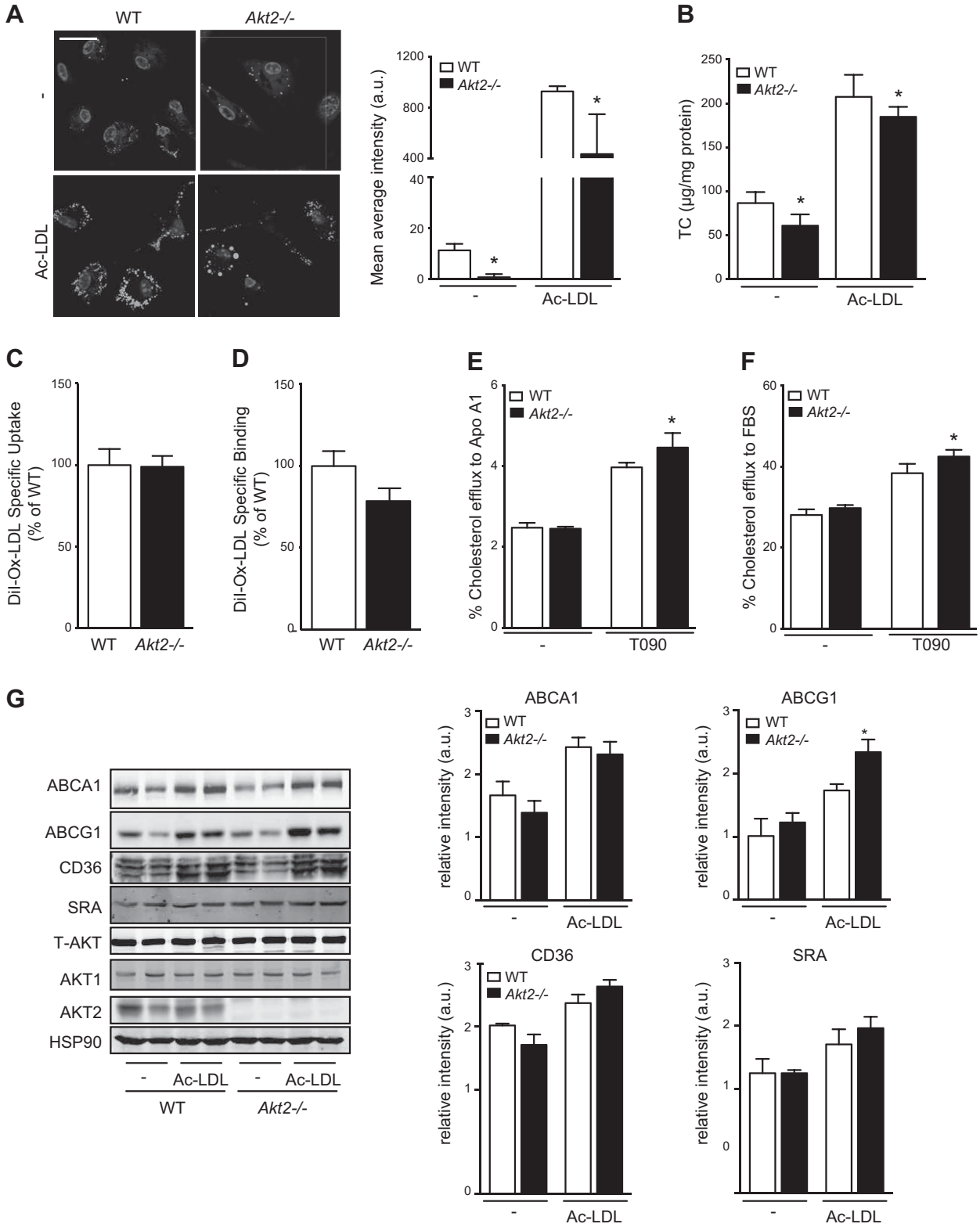

Figure 4. *Akt2*$^{-/-}$ peritoneal macrophages have less foam cell formation and increased cholesterol efflux. (*A*) Representative pictures from peritoneal macrophages incubated with or without Ac-LDL (120 μg/ml) for 24 h at 37°C. Following incubation, cells were washed, fixed, and stained with Bodipy 493/503 and DAPI (green and blue, respectively). Scale bar, 5 μm. Right panel, data are the mean ± SEM and representative of ≥3 experiments in duplicate. (*B*) Total cholesterol content in peritoneal macrophages from WT and *Akt2*$^{-/-}$ incubated with or without Ac-LDL for 24 h. (*C*) Flow cytometry analysis of DiI-Ox-LDL uptake in peritoneal macrophages incubated with DiI-Ox-LDL (30 μg/ml cholesterol) for 2 h at 37°C. (*D*) Flow cytometry analysis of Dil-Ox-LDL binding in peritoneal macrophages incubated with DiI-Ox-LDL (30 μg/ml cholesterol) for 1 h and 30 min at 4°C. At the end of the incubation period, cells were washed and incubated with 1 ml RPMI 1640 medium containing 10% fetal

(*continued on next page*)

MCP-1– and M-CSF–induced migration is impaired in *Akt2*$^{-/-}$ macrophages

Macrophage infiltration in the arterial wall in response to chemoattractants such as MCP-1 initiates the inflammatory response during atherogenesis. MCP-1 rapidly activates the PI3K/Akt signaling pathway, leading to monocyte recruitment in the arterial wall. Therefore, we assessed the role of Akt2 in macrophage migration in response to MCP-1 and M-CSF. As seen in Fig. 6*A*, the absence of Akt2 significantly reduced the response to both chemoattractants. Similar results were observed when BMDMs were loaded with cholesterol 24 h before the migration was assessed (Supplemental Fig. 4*C*). CCR2 regulates MCP-1–mediated macrophage migration. Thus, we wondered whether CCR2 expression levels were reduced in *Akt2*$^{-/-}$ BMDMs compared with WT BMDMs. Of note, the absence of Akt2 significantly reduces CCR2 expression in blood monocytes (Fig. 6*B*).

Rho GTPases such as Rac, RhoA, and Cdc42 are well known to play a crucial role in cell migration (25, 26). In particular, Rac1 has been linked to membrane ruffle/lamellipodia formation, with the highest concentrations of active Rac-1 located at the leading edge of motile cells (25, 26). Therefore, we analyzed the subcellular localization of Rac-1 in WT and *Akt2*$^{-/-}$ macrophages. Immunofluorescence analysis showed a significant reduction of Rac-1 localization in the plasma membrane in response to M-CSF in Akt2-deficient macrophages compared with WT macrophages (Fig. 6*C*). Moreover, filamentous actin (F-actin) staining that labels actin cytoskeleton structures critical for cell motility was significantly reduced in *Akt2*$^{-/-}$ macrophages. We further analyzed the Rac-1 activity in WT and *Akt2*$^{-/-}$ macrophages in response to M-CSF. As expected by its mislocalization, Rac-1 activation was markedly reduced in Akt2-deficient macrophages compared with WT macrophages (Fig. 6*D*). These results demonstrate that Akt2 is important in regulating the macrophage migratory response to the atherogenic cytokines MCP-1 and M-CSF.

Loss of Akt2 results in a reduction of AKT and PAK phosphorylation

To directly examine cellular substrates that may explain the impaired migratory response of macrophages, we assessed Akt substrate phosphorylation (PAK, GSK3, and FoxO1) in response to M-CSF stimulation in BMDMs. The results showed that loss of Akt2 results in a modest reduction of the phosphorylation of AKT, PAK, and ERK at early time points (2 min) (Fig. 6*E*). The phosphorylation of other Akt substrates, including FoxO1 and GSK3, was similar between both groups of macrophages.

DISCUSSION

The Akt family of proteins regulates cell growth and survival and cell metabolism (27). A growing body of literature has illustrated that individual members of Akt family proteins have different biological functions (11–13). We previously demonstrated that Akt1 plays a major role in controlling endothelial cell functions. Indeed, absence of Akt1 results in impaired angiogenesis, acute inflammatory response, and severe atherosclerosis (4, 5, 14, 15). Although the role of Akt1 during the progression of several cardiovascular diseases such as atherosclerosis, pathologic angiogenesis, and cardiac hypertrophy is very well established, the importance of other Akt isoforms remains to be fully characterized (4, 5, 14, 15). In the present work, we show that the absence of Akt2 does not influence the progression of atherosclerosis in mice. This result was unexpected because *Akt2*$^{-/-}$ *Ldlr*$^{-/-}$ mice develop hyperglycemia, dyslipidemia, and insulin resistance. We found it intriguing that Akt2 is a critical regulator of macrophage migration, lipid accumulation, and inflammation. BMT experiments directly demonstrated that the genetic ablation of Akt2 protects against the progression of atherosclerosis. This finding strongly suggests that, although systemic inhibition of Akt2 might be detrimental for avoiding the progression of atherosclerosis, macrophage-specific Akt2 targeting could be useful for treating this vascular disease.

During the preparation of this article, a report published that *Akt2*$^{-/-}$*Ldlr*$^{-/-}$ mice display impaired glucose tolerance and develop more complex atherosclerotic plaques than *Ldlr*$^{-/-}$ mice (28). Although the effect observed in plaque size was similar to the results reported in our study, we were not able to find significant alterations in the atherosclerotic plaque morphology between both groups of mice. These contradictory results can be explained because the plaque formation was induced by perivascular collar placement and mice were placed on Western diet (0.25% cholesterol) for a total of 8 wk, whereas we fed mice an HC diet (1.25% cholesterol) for 12 wk. Another important difference between both studies is the analysis of the contribution of hematopoietic cells during the progression of atherosclerosis. Although the previous study did not assess the role of hematopoietic cells during atherogenesis, we directly demonstrate that the absence of *Akt2*$^{-/-}$ in bone marrow-derived cells markedly reduces atherosclerotic plaque formation in mice. Although these results strongly suggest a major contribution of Akt2 in hematopoietic cells during the progression of atherosclerosis, we cannot rule out the potential role of Akt2 in the vascular wall during atherogenesis. Further BMT studies will be important to determine the relative contribution of Akt2 in bone marrow-derived cells and in the vascular wall during the progression of this disease.

bovine serum for 15 min at 37°C to allow the internalization. The results are expressed in terms of specific median intensity of fluorescence after subtracting autofluorescence of cells incubated in the absence of DiI-Ox-LDL. Total cholesterol efflux to apolipoprotein A1 (ApoA1) (*E*) or fetal bovine serum (*F*) in peritoneal macrophages from WT and *Akt2*$^{-/-}$ stimulated with or without T0901317 (T090). (*G*) Western blot analysis of ABCA1, ABCG1, CD36, SRA, AKT, AKT1, and AKT2 expression in peritoneal macrophages from WT and *Akt2*$^{-/-}$ incubated with or without Ac-LDL for 24 h. HSP90 was used as a loading control. Band densitometry is shown in the right panels. Data are the mean ± SEM of 3 independent experiments performed in triplicate. $^{*}P < 0.05$ compared with WT.

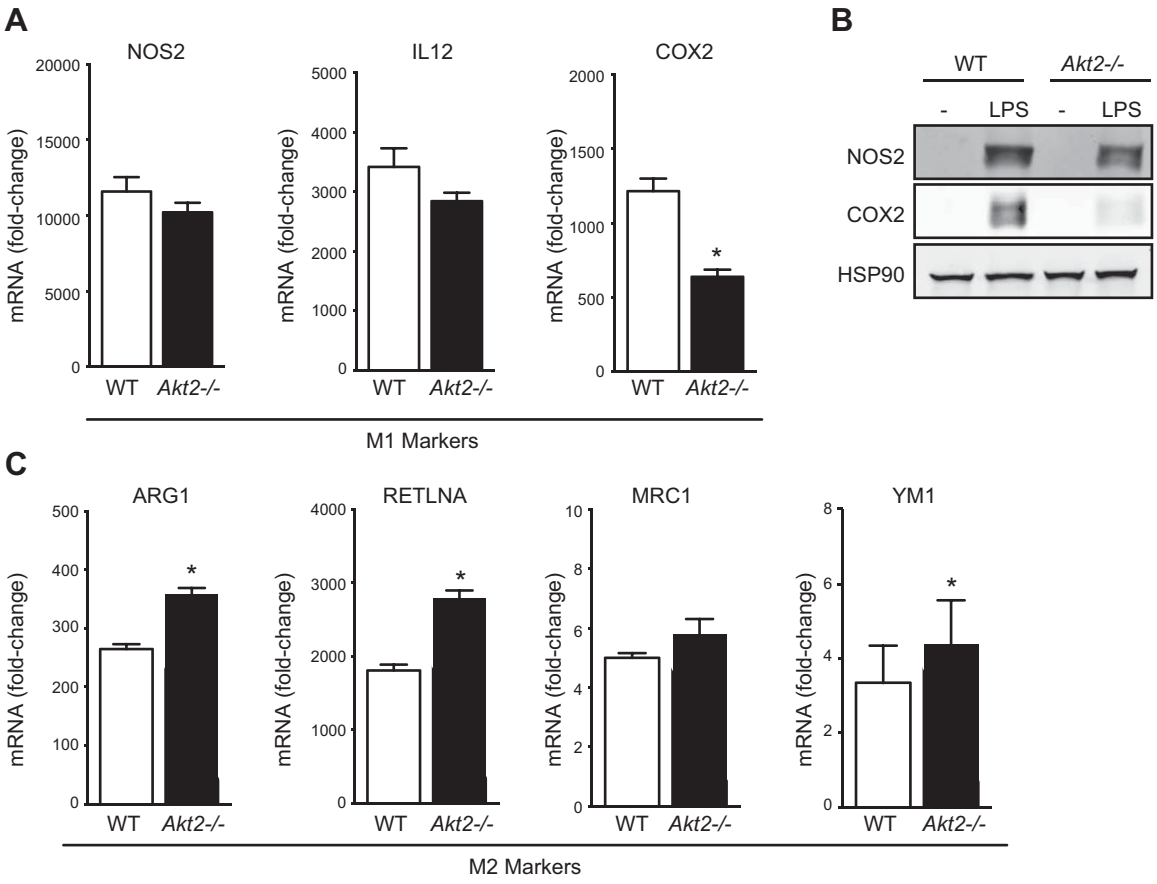

Figure 5. Akt2 deficiency results in alternative activated or M2 macrophages. (*A*) Gene expression of several M1 markers after stimulation with LPS (10 ng/ml) and IFN-γ (20 ng/ml). (*B*) Representative Western blot analysis of NOS2, COX2, and HSP90 expression in WT and $Akt2^{-/-}$ macrophages treated with LPS (10 ng/ml) and IFN-γ (20 ng/ml) for 8 h. Similar results were observed in 3 independent experiments. (*C*) Gene expression of several M2 markers after stimulation with IL-4 (15 ng/ml). $^*P < 0.05$ compared with WT.

To investigate the mechanism involved in the atheroprotection observed in $Ldlr^{-/-}$ mice transplanted with $Akt2^{-/-}$-deficient bone marrow, we assessed the proatherogenic processes associated with macrophages during the progression of atherosclerosis such as *1*) macrophage foam cell formation, *2*) macrophage migration, and *3*) macrophage inflammatory response. The role of Akt in regulating cholesterol accumulation in macrophages was previously studied in mice lacking Akt1 and Akt3 (4, 29). Although $Akt1^{-/-}$ macrophages tend to accumulate less cholesterol, deletion of *Akt3* promotes macrophage cholesterol accumulation and foam cell formation *in vitro* (4, 29). Mechanistically, Akt3 deficiency increases acetyl-coenzyme A acetyltransferase 1 expression, an enzyme involved in cholesterol esterification and accumulation in lipid droplets, and lipoprotein uptake (29). In contrast, our results showed that absence of Akt2 reduces foam cell formation *in vitro*. We found that $Akt2^{-/-}$ macrophages have similar binding and uptake of modified lipoproteins but have slightly enhanced cellular cholesterol efflux. Western blot analysis revealed a small but consistent increase in ABCG1 but not in ABCA1. Despite this observation, we cannot rule out that Akt2 could affect ABCA1 protein localization and activity. Indeed, a recent report recently demonstrated that the PI3K/Akt signaling pathway mediates the posttranscriptional regulation of ABCA1 and ABCG1 by controlling their intracellular localization (30). These observations suggest that the Akt signaling pathway regulates lipid metabolism in macrophages. Interestingly, different Akt isoforms regulate lipid accumulation in the opposite manner. Therefore, further experimentation is required to determine the specific substrate for each isoform that regulates lipid metabolism in macrophages. Moreover, it will also be important to assess whether the genetic loss of individual Akt genes regulates the activity and expression of other Akt family members in macrophages.

Macrophage infiltration into the arterial wall induces the development of early atherosclerotic lesions (20, 24). Several chemoattractants, such as MCP-1 and M-CSF, mediate the accumulation of macrophages in the arteries in response to injury (20, 24). Both cytokines stimulate the PI3K/Akt signaling pathway and regulate actin cytoskeleton changes required for cell migration (31). The role of Akt kinases in cell migration seems to be cell type specific. Although Akt1 and Akt2 appear to be required for vascular smooth muscle cell migration (5, 28), both isoforms play opposing roles in regulating fibroblast migration (32). In our study, we found that $Akt2^{-/-}$ is required for macrophage chemotaxis in response to MCP-1 and M-CSF, and its absence results in a significant reduction of macrophage accumulation in mouse

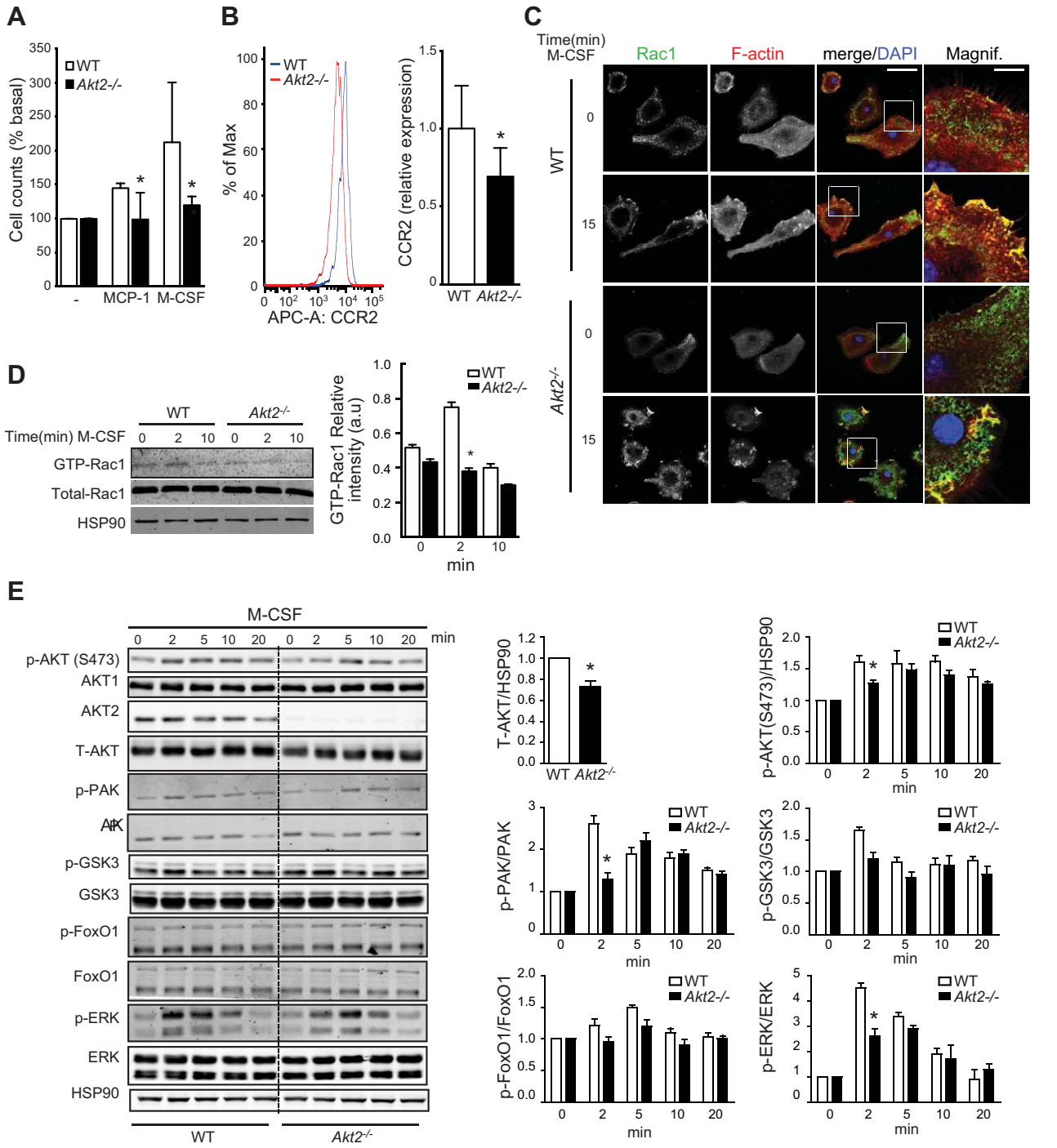

Figure 6. *Akt2*$^{-/-}$ BMDMs have less cell migration, Rac localization, and activation. (*A*) Migration of BMDMs from adult male WT or *Akt2*$^{-/-}$ mice was examined using transwells after stimulation with serum-free DMEM (0% fetal bovine serum) and MCP-1 (100 ng/ml) or M-CSF (100 ng/ml) for 16 h. The data represent the mean ± SEM of 4 independent experiments performed in triplicate. *$P < 0.05$ compared with WT BMDM cells. (*B*) Flow cytometry analysis of CCR2 expression in blood monocytes isolated from WT and *Akt2*$^{-/-}$ mice. Quantitative analysis ($n = 5$ mice each group) is represented in the right panel. *$P < 0.05$ compared with WT blood monocytes. (*C*) Representative confocal images of BMDMs isolated from adult male WT or *Akt2*$^{-/-}$ mice starved overnight and treated with M-CSF (50 ng/ml). At indicated time points, cells were fixed and stained with Rac1 (green), F-actin (red), and DAPI (blue). Scale bar, 10 μm. Inset scale bar, 5 μm. (*D*) Western blot analysis for active Rac indicates impaired kinetics of Rac activation on M-CSF activation. Similar results were observed in 2 independent experiments *$P < 0.05$ compared with WT BMDM cells. (*E*) Substrate specificity of Akt2 in BMDM. Immunoblots of BMDMs from adult male *WT* or *Akt2*$^{-/-}$ mice stimulated with M-CSF (50 ng/ml) at different time points. HSP90 was used as a loading control. Band densitometry is shown in the right panels. Data correspond to a representative Western blot analysis of 3 independent experiments that gave similar results. *$P < 0.05$ compared with WT BMDM cells.

atherosclerotic plaques. Similar results were previously reported using THP-1 cells, a human monocytic cell line (33). The role of Akt2 in controlling cellular migration has also been studied in neutrophils (34). In accordance with the results reported here, *Akt2*$^{-/-}$ neutrophils exhibited decreased cell migration compared with WT and *Akt1*$^{-/-}$ neutrophils (35). These results suggest that the Akt isoforms are not redundant but rather have specific functions in different cell types. We further analyzed the mechanism by which Akt2 deficiency results in impaired macrophage migration. To this end, we explored Rac-1 localization and activity after MCP-1 stimulation. Rac-1 is localized at the leading edge of motile cells in response to a chemoattractant. It is noteworthy that we found that Rac-1 is mislocalized in Akt2-deficient macrophages in response to MCP-1. Moreover, we observed a significant reduction of Rac-1 activation, suggesting that Akt2 is important for controlling Rac-1 activation in macrophages.

Plaque microenvironment regulates macrophage inflammatory responses (24). It has been proposed that macrophages might be polarized into two inflammatory statuses: M1 or proinflammatory macrophages and M2 or alternative activated macrophages. Although M1 macrophages are associated with promoting plaque inflammation, M2 macrophages are linked with resolving plaque inflammation, thus promoting atherosclerotic plaque regression. Interestingly, we found that Akt2 deficiency results in an M2 type phenotype *in vitro*. Likewise, Tsatsanis laboratory recently demonstrated that *Akt2*$^{-/-}$ macrophage polarize to an M2 type phenotype (18). Accordingly, Akt2-deficient mice are more resistant to LPS-induced endotoxin shock than WT and *Akt1*$^{-/-}$ mice (18). These findings and the results provided in this study suggest that Akt2 might protect against the progression of atherosclerosis by hampering inflammation within the atherosclerotic plaques.

Although these results demonstrate that Akt2 plays an important role in controlling macrophage functions *in vitro*, the phenotype we observed *in vivo* could be more complex because Akt2 may also regulate biological functions in other bone marrow-derived cells, such as neutrophils, B cells, and T lymphocytes, which influence the progression of atherosclerosis. In this regard, it has recently been shown that Akt2-deficient neutrophils exhibit decreased cell migration, granule enzyme release, and decreased O_2^- production compared with WT neutrophils (35). Moreover, Akt2 also plays an important role in controlling T- and B-cell functions. Given the prominent role of macrophages during the progression of atherosclerosis, we decided to focus our study on the contribution of Akt2 in macrophages during atherogenesis. However, further studies using tissue-specific Akt2-null mouse models are warranted to understand the relative contribution of other hematopoietic-derived cells during atherogenesis.

In conclusion, our study demonstrates that Akt2 regulates multiple macrophage functions including lipid metabolism, inflammation, and migration. Moreover, we uncover the role for this kinase during the progression of atherosclerosis. These results also challenge an existing paradigm that the suppression of the Akt signaling pathway might worsen atherosclerotic vascular disease as shown in Akt1- and Akt3-deficient mice. It is surprising that macrophage-specific ablation of Akt2 confers a significant protection against the progression of atherosclerosis in mice. Further studies focusing on determining Akt substrate specificity will be required to fully understand the physiologic role of this family of kinases in controlling macrophage functions. Furthermore, this study suggests that specific Akt2 targeting in macrophages might be beneficial for treating atherosclerosis vascular disease. FJ

This work was supported by U.S. National Institutes of Health (NIH) National Heart, Lung, and Blood Institute Grants R01HL107953 and R01HL106063 (to C.F.-H.), R01HL105945 (to Y.S.), R01HL064793 and R01HL061371 (to W.C.S.), and NIH National Institute on Aging Grant 1F31AG043318 (to L.G); a grant from the Foundation Leducq Transatlantic Network of Excellence (to C.F.-H. and W.C.S.); a postdoctoral fellowship from the Spanish Ministry (Programa Nacional de Movilidad de Recursos Humanos del Plan Nacional de I-D+i 2008-2011) (to N.R.); American Heart Association Grant 12POST9780016 (to C.M.R.); a Howard Hughes Medical Institute International Student Research Fellowship (to E.A.); and the Capes Foundation, Ministry of Education of Brazil, Brazil (to A.G.S. and A.C.W.).

REFERENCES

1. Bornfeldt, K. E., and Tabas, I. (2011) Insulin resistance, hyperglycemia, and atherosclerosis. *Cell Metab.* **14**, 575–585
2. Tabas, I., Tall, A., and Accili, D. (2010) The impact of macrophage insulin resistance on advanced atherosclerotic plaque progression. *Circ. Res.* **106**, 58–67
3. Cohen, D. E., and Fisher, E. A. (2013) Lipoprotein metabolism, dyslipidemia, and nonalcoholic fatty liver disease. *Semin. Liver Dis.* **33**, 380–388
4. Fernández-Hernando, C., Ackah, E., Yu, J., Suárez, Y., Murata, T., Iwakiri, Y., Prendergast, J., Miao, R. Q., Birnbaum, M. J., and Sessa, W. C. (2007) Loss of Akt1 leads to severe atherosclerosis and occlusive coronary artery disease. *Cell Metab.* **6**, 446–457
5. Fernández-Hernando, C., József, L., Jenkins, D., Di Lorenzo, A., and Sessa, W. C. (2009) Absence of Akt1 reduces vascular smooth muscle cell migration and survival and induces features of plaque vulnerability and cardiac dysfunction during atherosclerosis. *Arterioscler. Thromb. Vasc. Biol.* **29**, 2033–2040
6. Han, S., Liang, C. P., DeVries-Seimon, T., Ranalletta, M., Welch, C. L., Collins-Fletcher, K., Accili, D., Tabas, I., and Tall, A. R. (2006) Macrophage insulin receptor deficiency increases ER stress-induced apoptosis and necrotic core formation in advanced atherosclerotic lesions. *Cell Metab.* **3**, 257–266
7. Rask-Madsen, C., Li, Q., Freund, B., Feather, D., Abramov, R., Wu, I. H., Chen, K., Yamamoto-Hiraoka, J., Goldenbogen, J., Sotiropoulos, K. B., Clermont, A., Geraldes, P., Dall'Osso, C., Wagers, A. J., Huang, P. L., Rekhter, M., Scalia, R., Kahn, C. R., and King, G. L. (2010) Loss of insulin signaling in vascular endothelial cells accelerates atherosclerosis in apolipoprotein E null mice. *Cell Metab.* **11**, 379–389
8. Tsuchiya, K., Tanaka, J., Shuiqing, Y., Welch, C. L., DePinho, R. A., Tabas, I., Tall, A. R., Goldberg, I. J., and Accili, D. (2012) FoxOs integrate pleiotropic actions of insulin in vascular endothelium to protect mice from atherosclerosis. *Cell Metab.* **15**, 372–381
9. Bae, S. S., Cho, H., Mu, J., and Birnbaum, M. J. (2003) Isoform-specific regulation of insulin-dependent glucose uptake by Akt/protein kinase B. *J. Biol. Chem.* **278**, 49530–49536
10. Leavens, K. F., and Birnbaum, M. J. (2011) Insulin signaling to hepatic lipid metabolism in health and disease. *Crit. Rev. Biochem. Mol. Biol.* **46**, 200–215
11. Cho, H., Mu, J., Kim, J. K., Thorvaldsen, J. L., Chu, Q., Crenshaw III, E. B., Kaestner, K. H., Bartolomei, M. S., Shulman, G. I., and Birnbaum, M. J. (2001) Insulin resistance and a diabetes mellitus-like syndrome in mice lacking the protein kinase Akt2 (PKB beta). *Science* **292**, 1728–1731

12. Cho, H., Thorvaldsen, J. L., Chu, Q., Feng, F., and Birnbaum, M. J. (2001) Akt1/PKBalpha is required for normal growth but dispensable for maintenance of glucose homeostasis in mice. *J. Biol. Chem.* **276**, 38349–38352
13. Easton, R. M., Cho, H., Roovers, K., Shineman, D. W., Mizrahi, M., Forman, M. S., Lee, V. M., Szabolcs, M., de Jong, R., Oltersdorf, T., Ludwig, T., Efstratiadis, A., and Birnbaum, M. J. (2005) Role for Akt3/protein kinase Bgamma in attainment of normal brain size. *Mol. Cell. Biol.* **25**, 1869–1878
14. Ackah, E., Yu, J., Zoellner, S., Iwakiri, Y., Skurk, C., Shibata, R., Ouchi, N., Easton, R. M., Galasso, G., Birnbaum, M. J., Walsh, K., and Sessa, W. C. (2005) Akt1/protein kinase Balpha is critical for ischemic and VEGF-mediated angiogenesis. *J. Clin. Invest.* **115**, 2119–2127
15. Chen, J., Somanath, P. R., Razorenova, O., Chen, W. S., Hay, N., Bornstein, P., and Byzova, T. V. (2005) Akt1 regulates pathological angiogenesis, vascular maturation and permeability in vivo. *Nat. Med.* **11**, 1188–1196
16. Shiojima, I., Sato, K., Izumiya, Y., Schiekofer, S., Ito, M., Liao, R., Colucci, W. S., and Walsh, K. (2005) Disruption of coordinated cardiac hypertrophy and angiogenesis contributes to the transition to heart failure. *J. Clin. Invest.* **115**, 2108–2118
17. González-Navarro, H., Vinué, A., Vila-Caballer, M., Fortuño, A., Beloqui, O., Zalba, G., Burks, D., Díez, J., and Andrés, V. (2008) Molecular mechanisms of atherosclerosis in metabolic syndrome: role of reduced IRS2-dependent signaling. *Arterioscler. Thromb. Vasc. Biol.* **28**, 2187–2194
18. Arranz, A., Doxaki, C., Vergadi, E., Martinez de la Torre, Y., Vaporidi, K., Lagoudaki, E. D., Ieronymaki, E., Androulidaki, A., Venihaki, M., Margioris, A. N., Stathopoulos, E. N., Tsichlis, P. N., and Tsatsanis, C. (2012) Akt1 and Akt2 protein kinases differentially contribute to macrophage polarization. *Proc. Natl. Acad. Sci. USA* **109**, 9517–9522
19. Vergadi, E., Vaporidi, K., Theodorakis, E. E., Doxaki, C., Lagoudaki, E., Ieronymaki, E., Alexaki, V. I., Helms, M., Kondili, E., Soennichsen, B., Stathopoulos, E. N., Margioris, A. N., Georgopoulos, D., and Tsatsanis, C. (2014) Akt2 deficiency protects from acute lung injury via alternative macrophage activation and miR-146a induction in mice. *J. Immunol.* **192**, 394–406
20. Glass, C. K., and Witztum, J. L. (2001) Atherosclerosis. the road ahead. *Cell* **104**, 503–516
21. Lusis, A. J. (2000) Atherosclerosis. *Nature* **407**, 233–241
22. Locati, M., Mantovani, A., and Sica, A. (2013) Macrophage activation and polarization as an adaptive component of innate immunity. *Adv. Immunol.* **120**, 163–184
23. Martinez, F. O., Gordon, S., Locati, M., and Mantovani, A. (2006) Transcriptional profiling of the human monocyte-to-macrophage differentiation and polarization: new molecules and patterns of gene expression. *J. Immunol.* **177**, 7303–7311
24. Moore, K. J., Sheedy, F. J., and Fisher, E. A. (2013) Macrophages in atherosclerosis: a dynamic balance. *Nat. Rev. Immunol.* **13**, 709–721
25. Ridley, A. J. (2008) Regulation of macrophage adhesion and migration by Rho GTP-binding proteins. *J. Microsc.* **231**, 518–523
26. Ridley, A. J. (2011) Life at the leading edge. *Cell* **145**, 1012–1022
27. Manning, B. D., and Cantley, L. C. (2007) AKT/PKB signaling: navigating downstream. *Cell* **129**, 1261–1274
28. Rensing, K. L., de Jager, S. C., Stroes, E. S., Vos, M., Twickler, M. T., Dallinga-Thie, G. M., de Vries, C. J., Kuiper, J., Bot, I., and von der Thüsen, J. H. (2014) Akt2/LDLr double knockout mice display impaired glucose tolerance and develop more complex atherosclerotic plaques than LDLr knockout mice. *Cardiovasc. Res.* **101**, 277–287
29. Ding, L., Biswas, S., Morton, R. E., Smith, J. D., Hay, N., Byzova, T. V., Febbraio, M., and Podrez, E. A. (2012) Akt3 deficiency in macrophages promotes foam cell formation and atherosclerosis in mice. *Cell Metab.* **15**, 861–872
30. Huang, C. X., Zhang, Y. L., Wang, J. F., Jiang, J. Y., and Bao, J. L. (2013) MCP-1 impacts RCT by repressing ABCA1, ABCG1, and SR-BI through PI3K/Akt posttranslational regulation in HepG2 cells. *J. Lipid Res.* **54**, 1231–1240
31. Gerszten, R. E., Friedrich, E. B., Matsui, T., Hung, R. R., Li, L., Force, T., and Rosenzweig, A. (2001) Role of phosphoinositide 3-kinase in monocyte recruitment under flow conditions. *J. Biol. Chem.* **276**, 26846–26851
32. Zhou, G. L., Tucker, D. F., Bae, S. S., Bhatheja, K., Birnbaum, M. J., and Field, J. (2006) Opposing roles for Akt1 and Akt2 in Rac/Pak signaling and cell migration. *J. Biol. Chem.* **281**, 36443–36453
33. Zhang, B., Ma, Y., Guo, H., Sun, B., Niu, R., Ying, G., and Zhang, N. (2009) Akt2 is required for macrophage chemotaxis. *Eur. J. Immunol.* **39**, 894–901
34. Li, J., Kim, K., Hahm, E., Molokie, R., Hay, N., Gordeuk, V. R., Du, X., and Cho, J. (2014) Neutrophil AKT2 regulates heterotypic cell-cell interactions during vascular inflammation. *J. Clin. Invest.* **124**, 1483–1496
35. Chen, J., Tang, H., Hay, N., Xu, J., and Ye, R. D. (2010) Akt isoforms differentially regulate neutrophil functions. *Blood* **115**, 4237–4246

Received for publication July 29, 2014.
Accepted for publication September 26, 2014.